



Journal of Agrometeorology

(A publication of Association of Agrometeorologists)

ISSN : 0972-1665 (print), 2583-2980 (online)

Vol. No. 28 (1) : 80 - 87 (March - 2026)

<https://doi.org/10.54386/jam.v28i1.3309>

<https://journal.agrimetassociation.org/index.php/jam>



Research paper

Prototype framework for agricultural drought monitoring in Northern Thailand using Satellite-based evaporative stress index

N. BOONPIN^{1,2}, P. WAIPHARA² and C. CHOMPUCHAN^{2*}

¹Northern Royal Rainmaking Operation Center, Tak 63000, Thailand

²Department of Irrigation Engineering, Faculty of Engineering at Kamphaeng Saen, Kasetsart University (Kamphaeng Saen Campus), Nakhon Pathom 73140, Thailand

*Corresponding Author: fengcpc@ku.ac.th <https://orcid.org/0000-0001-8402-6811>

ABSTRACT

Agricultural drought threatens crop production in Northern Thailand, where complex terrain and limited meteorological stations restrict effective ground-based monitoring. This study developed a prototype framework for agricultural drought monitoring using the satellite-based Evaporative Stress Index (ESI). Bias-corrected reference evapotranspiration (ET_o) from TerraClimate was combined with satellite-derived actual evapotranspiration (ET_a) from SSEBop to calculate 10-day ESI values during 2012–2023. A classification system based on consecutive ESI patterns was developed to generate action-oriented maps for emergency response. Temporal analysis revealed persistent agricultural drought from late 2021 through early 2022. Spatial analysis identified significant heterogeneity across the region, revealing localized stress areas that regional averages failed to detect. The consecutive-period classification prioritized areas under constant stress requiring emergency intervention over those experiencing only temporary fluctuations. Overall, the proposed prototype framework provides decision-support capabilities that can be integrated with exposure and resistance factors to guide resource allocation in regions with sparse ground-based monitoring infrastructure.

Keywords: Agricultural drought, Evaporative Stress Index, drought monitoring, Northern Thailand, Remote sensing, Satellite-based assessment

Agricultural drought critically impacts food security by limiting water availability during essential crop growth stages. In tropical regions, rapid onset (within weeks) leaves insufficient adaptation time, resulting in major yield losses (Otkin *et al.*, 2013) and limiting traditional monitoring effectiveness. Agricultural drought monitoring in Southeast Asia faces limitations when relying on conventional indices such as the Standardized Precipitation Index (SPI), Standardized Precipitation Evapotranspiration Index (SPEI), and Palmer Drought Severity Index (PDSI) (Zaki & Noda, 2022). These indices are typically computed using a coarser temporal scale (such as 1-month or 3-month intervals) and are primarily designed to detect long-term drought events. For example, multiple timescales SPI analysis (SPI3–SPI12) shown that drought magnitude, duration, and frequency fluctuate significantly across temporal scales, especially during El Niño years (Mergia, 2024). Consequently, they may not accurately reflect actual crop water stress (Sreeparvathy *et al.*, 2025).

The Evaporative Stress Index (ESI) offers distinct advantages for agricultural drought detection by directly assessing vegetation water stress. ESI quantifies the reduction in transpiration rates using satellite-derived surface temperature, enabling crop stress detection before visible symptoms appear (Anderson *et al.*, 2007). This physiological response occurs within days of water limitation, enabling identification of agricultural drought during its development rather than after impacts become severe. Previous research by Yoon *et al.*, (2020) has demonstrated the effectiveness of ESI as an early agricultural stress indicator, particularly when management interventions remain most effective.

Given the need to monitor crop drought indicators, regions with complex terrain and limited in situ observations present an additional challenge for effective agricultural drought monitoring. Northern Thailand, with its complex mountainous terrain and limited meteorological stations, represents a region

Article info - DOI: <https://doi.org/10.54386/jam.v28i1.3309>

Received: 18 December 2025; Accepted: 17 January 2026; Published online : 1 March 2026

“This work is licensed under Creative Common Attribution-Non Commercial-ShareAlike 4.0 International (CC BY-NC-SA 4.0) © Author (s)”

where agricultural drought monitoring presents major challenges. This study developed a prototype framework for agricultural drought monitoring in Northern Thailand using satellite-based ESI. The objectives were to (1) characterize temporal and spatial drought patterns across Northern Thailand during 2012–2023 and (2) develop action-oriented mapping approaches suitable for operational implementation. The proposed framework demonstrates how satellite-based drought indices can be translated into practical decision-support tools for water management and emergency response organizations in regions with limited ground-based monitoring infrastructure.

MATERIALS AND METHODS

Study Location

The study area encompasses Northern Thailand, as defined by the meteorological regional classification, comprising 15 provinces with a total area of approximately 93,690 km² (Fig. 1). The topography consists predominantly of forests and high mountains interspersed with intermontane valleys and lowland plains. Altitudes range from 100 to 2,500 m above sea level. The climate is tropical monsoon with an average annual temperature of 20–34 °C and annual rainfall of 600–1,000 mm (Trisurat *et al.*, 2010).

Data Sources

Weather data from seven TMD (Thai Meteorological Department) stations across Northern Thailand were used in this study (Fig. 1). The data covered the period from 2012 to 2023 and

were used exclusively as reference data for bias correction of gridded ETo data. Gridded ETo data were obtained from TerraClimate, which provides monthly climate data with approximately 4 km spatial resolution covering the period from 1958 to present (Abatzoglou *et al.*, 2018). ETo values in TerraClimate are calculated using the Penman-Monteith equation. To minimize systematic bias, Quantile Mapping bias correction was applied using the Gumbel distribution, following established methodologies (Fang *et al.*, 2015). The bias correction procedure used pooled data from all seven meteorological stations to develop transfer functions for the entire study region. The bias-corrected ETo data were then used for ESI calculation.

ETa data were obtained from SSEBop (Operational Simplified Surface Energy Balance), an energy balance model developed by the US Geological Survey. SSEBop provides estimated ETa at 1 km spatial resolution with 10-day (decadal) temporal frequency. ETa is derived from the relationship between surface temperature and evaporative demand (Senay *et al.*, 2013). This satellite-derived ETa serves as the primary indicator of vegetation stress and forms the foundation of the ESI monitoring framework.

ESI Calculation

The ESI was calculated following the methodology developed by Anderson *et al.*, (2007), beginning with the calculation of the Evaporative Stress Ratio (ESR), which represents the ratio between ETa and ETo for each 10-day period, expressed as:

$$ESR = \frac{ETa}{ETo} \tag{1}$$

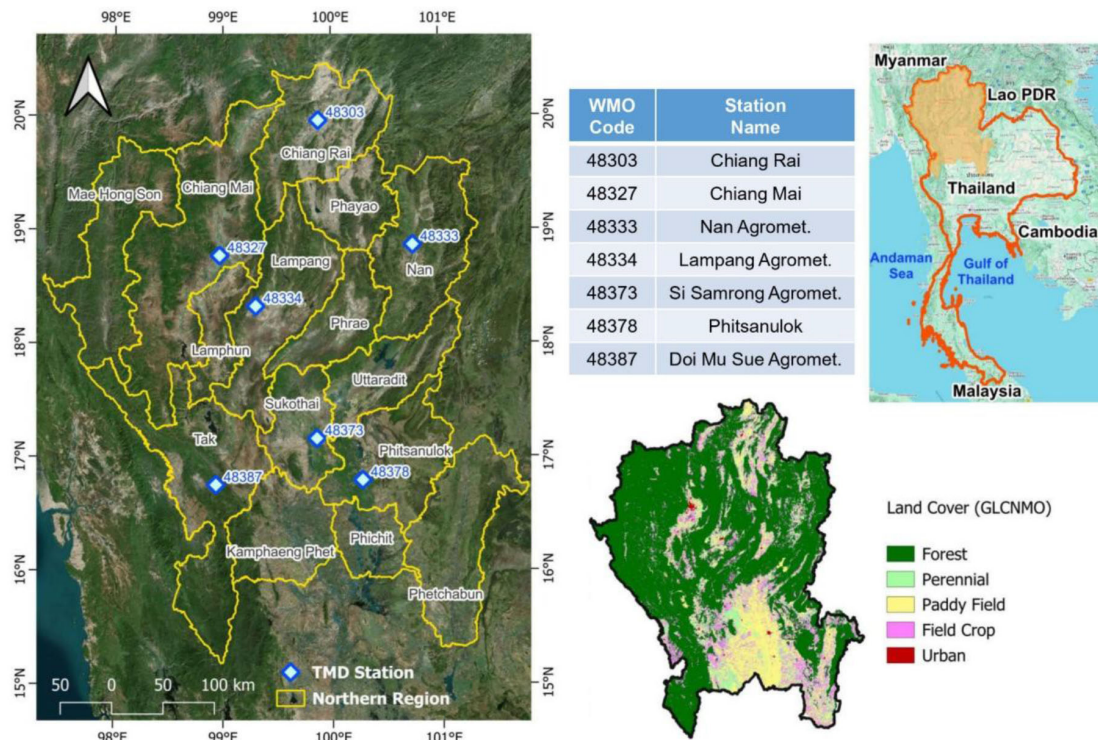


Fig. 1: Study area of Northern Thailand, including provincial boundaries, topography, and the distribution of meteorological stations

Table 1: Weighting system for ESI-CD and ESI-PD

Condition	ESI-CD	ESI-PD
Wet (ESI > 0.5)	10	1
Normal (-0.5 ≤ ESI ≤ 0.5)	20	2
Dry (ESI < -0.5)	30	3

Table 2: Drought severity classification based on combined scores

Combined Score	Severity Level	Pattern Type	Action Required
11-20	Level 1	No Stress	Regular Monitoring
21-30	Level 2	Transitional	Careful Monitoring
31-32	Level 3	Emerging Stress	Prepare Response
33	Level 4	Persistent Stress	Emergency Response

where ESR is the evaporative stress ratio, ET_a is actual evapotranspiration, and ET_o is reference crop evapotranspiration. ESR values range from 0 (severe water stress) to approximately 1 (adequate water availability), with lower values indicating greater evaporative stress.

ESR values were then standardized to enable comparison of drought conditions across different times and locations. ESR anomalies were converted to standardized values expressed as Z-scores, calculated as:

$$ESI = \frac{ESR_i - \overline{ESR}}{\sigma_{ESR}} \quad (2)$$

where ESR_i is the evaporative stress ratio for period i , \overline{ESR} is the mean evaporative stress ratio, and σ_{ESR} is the standard deviation of ESR. The standardization procedure was applied separately for each grid cell using the entire 2012–2023 period as the reference baseline. This approach ensures that ESI values represent anomalies relative to the long-term conditions specific to each location. ESI values are standardized Z-scores (mean=0, SD=1), typically ranging between -3 and +3. Negative values indicate vegetation water stress, while positive values reflect above-normal moisture availability.

To evaluate the relationship between ESI and meteorological drought, SPEI-1 data derived from ERA5 reanalysis (Keune *et al.*, 2025) were obtained from the Global Drought Observatory (GDO) with 10-day temporal resolution matching ESI. Pearson correlation coefficients were calculated between ESI and SPEI-1 time series at each TMD station.

Development of the ESI-based Drought Severity Classification

Development of drought severity classification criteria utilized pattern analysis of ESI changes between two consecutive 10-day periods (decadal). The classification system considers ESI values for the current 10-day period (ESI-CD) and the previous 10-day period (ESI-PD) to identify both current conditions and temporal trends. The first step involved establishing ESI condition classification thresholds. Based on research examining standardized (Z-score) indices, normal conditions were defined within the range of -0.5 to 0.5 (Wang *et al.*, 2021). This study defined ESI values > 0.5 as wet conditions, $-0.5 \leq ESI \leq 0.5$ as normal conditions, and ESI

< -0.5 as dry conditions.

The weighting system was designed to emphasize current decade conditions over previous decade conditions, acknowledging that current status is of greater importance for operational emergency response decisions. Current 10-day conditions (ESI-CD) were assigned weights of 10, 20, or 30, while previous 10-day conditions (ESI-PD) were assigned weights of 1, 2, or 3. This 10:1 weighting ratio ensures that current decadal conditions dominate the overall classification, while previous decadal conditions provide context for temporal persistence. The detailed scoring system is shown in Table 1. Combined scores from ESI-CD and ESI-PD range from 11 (wet conditions in both periods) to 33 (dry conditions in both periods). Based on these combined scores, severity levels were classified into four levels, and response measures were assigned, as shown in Table 2.

RESULTS AND DISCUSSION

Temporal Analysis of Drought using ESI

The ESI analysis for the period 2012–2023 (Fig. 2) indicates that drought events occurred most frequently during the dry season, specifically from February to April. Droughts were also observed during the mid-rainy season (August–September) in certain years, indicating irregular rainfall distribution during critical cultivation periods that can severely impact yields. In this study, drought was defined as two or more consecutive 10-day periods with $ESI < -0.5$. Analysis of the ESI time series revealed distinctions between drought frequency and severity. Certain stations (e.g., Doi Mu Sue Agromet.) exhibited a high frequency of drought events, suggesting recurrent water stress. However, these events were not always the most severe in terms of magnitude or duration.

To understand the relationship between vegetation stress and meteorological conditions, a correlation analysis was conducted (Fig. 3). Correlation between ESI and SPEI-1 across seven stations ranged from $r = 0.17$ to $r = 0.46$ (mean = 0.32). This modest association is expected because ESI captures vegetation water-stress responses, whereas SPEI reflects climatic water balance. Consistent with this interpretation, Chang *et al.*, (2023) reported that ESI relates more strongly to plant functional variables (e.g., gross primary production and surface conductance) than to meteorological drought indices, indicating that ESI reflects physiological stress rather than climate anomalies alone.

Two distinct temporal patterns emerged: short-duration severe events in 2012, 2014, 2015, and 2017 contrasted with prolonged drought conditions during 2016 and 2019–2020. These prolonged droughts typically persist for three to five months (Ha *et al.*, 2023). The major extended episodes (2016, 2019–2020) coincided with El Niño and positive Indian Ocean Dipole (IOD) events (Nurdiati *et al.*, 2022). The most significant agricultural drought was identified as a persistent drought period spanning from late 2021 to early 2022. This event was particularly impactful due to its extended duration and cumulative stress on agricultural resources rather than a single-season anomaly. This finding is noteworthy because the period was dominated by a La Niña event, which typically brings wetter conditions to Southeast Asia.

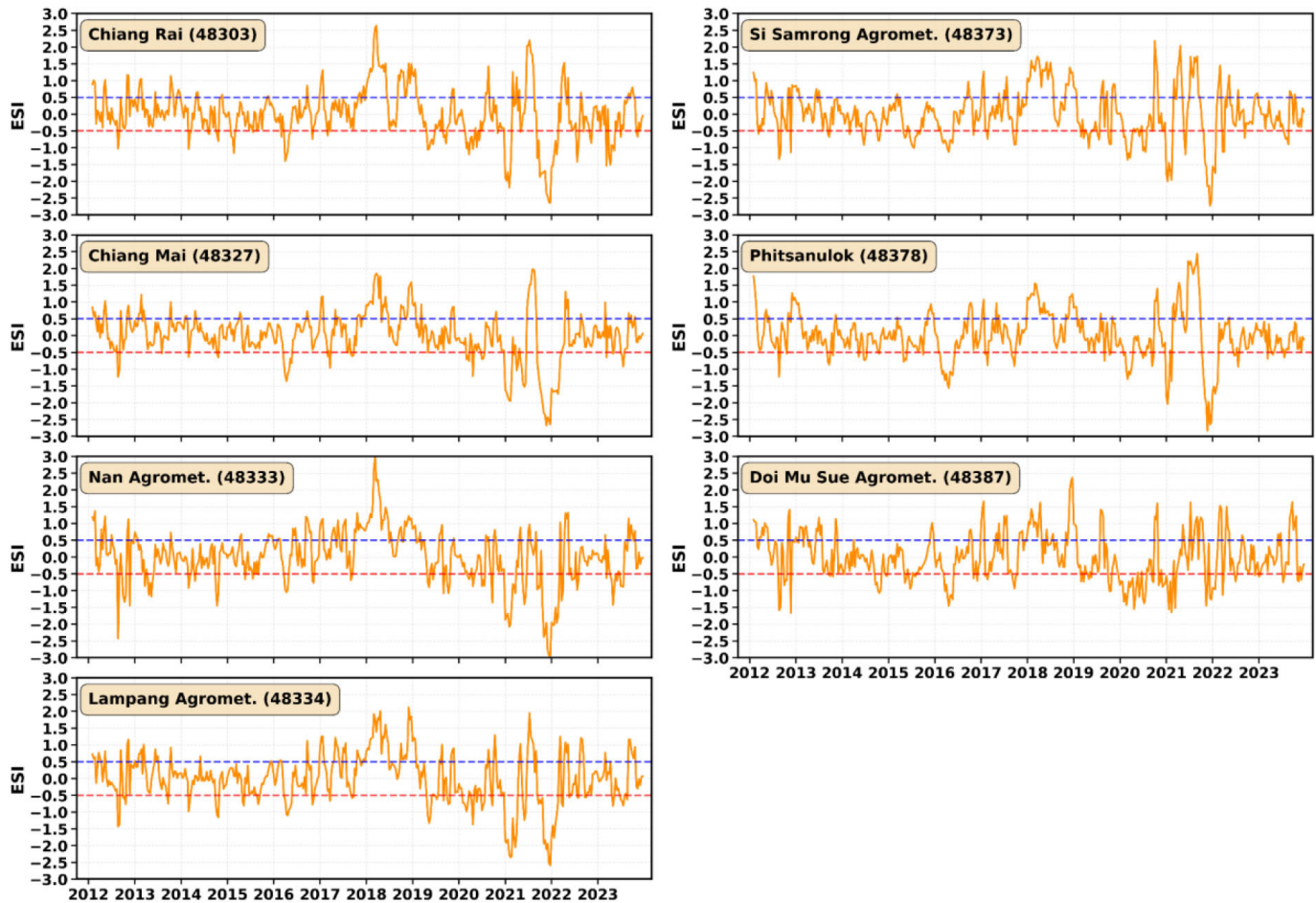


Fig. 2: Time series of ESI in Northern Thailand. Blue and red dash lines indicate the ESI threshold of wet and dry condition, respectively.

However, the agricultural stress detected by ESI aligns with ground-based observations. Despite La Niña, rainfall in 2021 was irregular, exhibiting clustered distribution patterns rather than widespread coverage, leading to recurring, localized agricultural drought and severe crop damage (Northern Meteorological Center, 2022). The ASMC Bulletin reported that Northern Thailand experienced below-average rainfall during January–March 2022 based on CHIRPS rainfall anomaly analysis against 1991–2020 climatology (ASEAN Specialised Meteorological Centre, 2022). Satellite-based analysis also reported similar findings regarding the severity of drought conditions in 2021 (Jeefoo, 2023). These reports provide independent verification of the ESI results.

The large-scale climate driver for this anomaly has been linked to the combined influence of La Niña and negative IOD conditions, which modulated regional circulation and was associated with abnormal atmospheric subsidence and rainfall suppression over parts of Northern Thailand (Jeong *et al.*, 2023). However, the severity of the 2021–2022 agricultural drought reflected complex interactions between meteorological conditions and water management. Agricultural drought developed despite La Niña because the upper northern region recorded below-normal rainfall even when national-scale rainfall totals were above normal (Hydro Informatics Institute, 2021). In the lower northern region, the main reservoirs of Bhumibol and Sirikit remained below

the lower rule curves through 2019–2021, severely constraining irrigation supply. Consequently, the Royal Irrigation Department (RID) encouraged farmers to reduce second-crop rice planting and promoted less water-intensive crops in affected provinces (USDA Foreign Agricultural Service, 2021). A lag of approximately 1–2 months commonly separates meteorological drought from agricultural drought because soil moisture depletion and plant stress accumulate after rainfall deficits. The persistent agricultural stress detected in late 2021 and early 2022 is consistent with cumulative rainfall deficits in preceding months, compounded by constrained irrigation supply and uneven rainfall distribution.

Spatial Distribution of ESI and Response Action Maps

The spatial analysis revealed significant variation in agricultural drought conditions across Northern Thailand. The gridded ESI data enabled the identification of localized drought hotspots even when regional averages appeared normal. Fig. 4 demonstrates the classification methodology through three February case studies representing different drought conditions: localized stress (2014), wet conditions (2018), and widespread drought (2022).

February 2014 illustrates the limitations of regional averaging. Despite normal area-averaged ESI (-0.5 to 0.5), northern

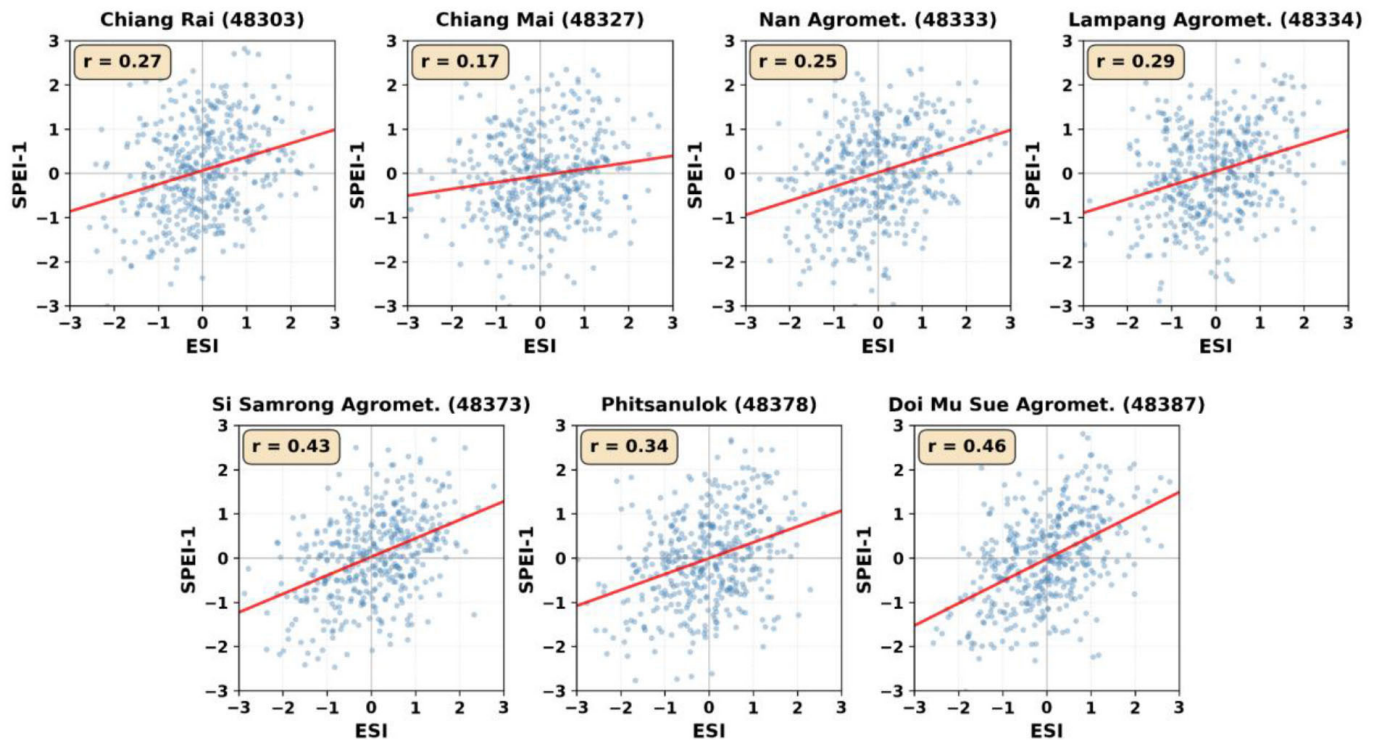


Fig. 3: Scatter plots showing the correlation between ESI and SPEI-1 across seven stations.

provinces (Chiang Rai, Nan) exhibited persistent stress ($ESI < -0.5$), triggering Level 4 classification. This demonstrates how regional averages mask localized hotspots requiring intervention.

In contrast, February 2018 presented uniformly favorable conditions throughout the study area, with ESI values exceeding 0.5 in both decadal periods indicating adequate soil moisture despite the dry season. The action-oriented map was dominated entirely by Level 1 (Regular Monitoring) with no areas requiring enhanced response measures. February 2022 demonstrates rapid spatial change tracking. Widespread stress during the second decadal improved in northern and southern provinces by the third decadal, while central provinces (Nan, Phrae, Phayao, Lampang, Lamphun) maintained persistent stress, triggering Level 4 classification. This enables targeted intervention to sustained stress areas rather than uniform regional responses.

The comparative analysis validates two fundamental strengths of the proposed methodology. First, the gridded ESI approach effectively detects localized water stress areas that regional averaging obscures. As Fig. 3 demonstrates, broad geographical domains exhibit considerable spatial heterogeneity in drought dynamics, particularly in progression rates, initiation timing, and persistence duration. Conventional area-averaging methods cannot adequately capture this spatial complexity, producing assessments that misrepresent actual conditions. This detection capability proves critical for directing emergency interventions toward severely stressed areas, even under apparently normal regional conditions. Second, the use of consecutive-period analysis enables prioritization based on temporal patterns rather than single-point conditions. Agricultural drought is characterized by sustained deficits in soil water content across multiple consecutive periods.

Research demonstrates that drought characteristics also differ across the temporal scale, with shorter-scale indices capturing brief wet-dry variabilities and longer timescales reflecting more persistent conditions (Yang et al., 2019). Accordingly, deficit duration across successive periods determines whether short-term stress develops into sustained drought requiring emergency intervention (Amazirh et al., 2023). This approach is particularly valuable in resource-limited contexts, where efficient allocation demands distinguishing temporary fluctuations from extended stress threatening agricultural production. The action-oriented maps support prioritization in disaster response planning by integrating drought severity with exposure level (crop vulnerability) and resistance capacity (irrigation availability, water storage, planning). Priority areas are characterized by high ESI stress, major crop exposure, and limited irrigation infrastructure (Pei et al., 2018).

Integration of the ESI-based framework with these factors would enable a comprehensive risk assessment. Areas classified as Level 4 (Persistent Stress) with high crop exposure and limited irrigation capacity represent the highest priority for emergency intervention. Conversely, areas with similar ESI classifications but adequate irrigation infrastructure may require different response strategies focused on optimizing water allocation rather than emergency relief. This integrated approach moves beyond simple hazard identification toward actionable risk assessment, supporting evidence-based decision-making for agricultural drought management.

CONCLUSION

This study developed a prototype agricultural drought monitoring framework for Northern Thailand using the satellite-

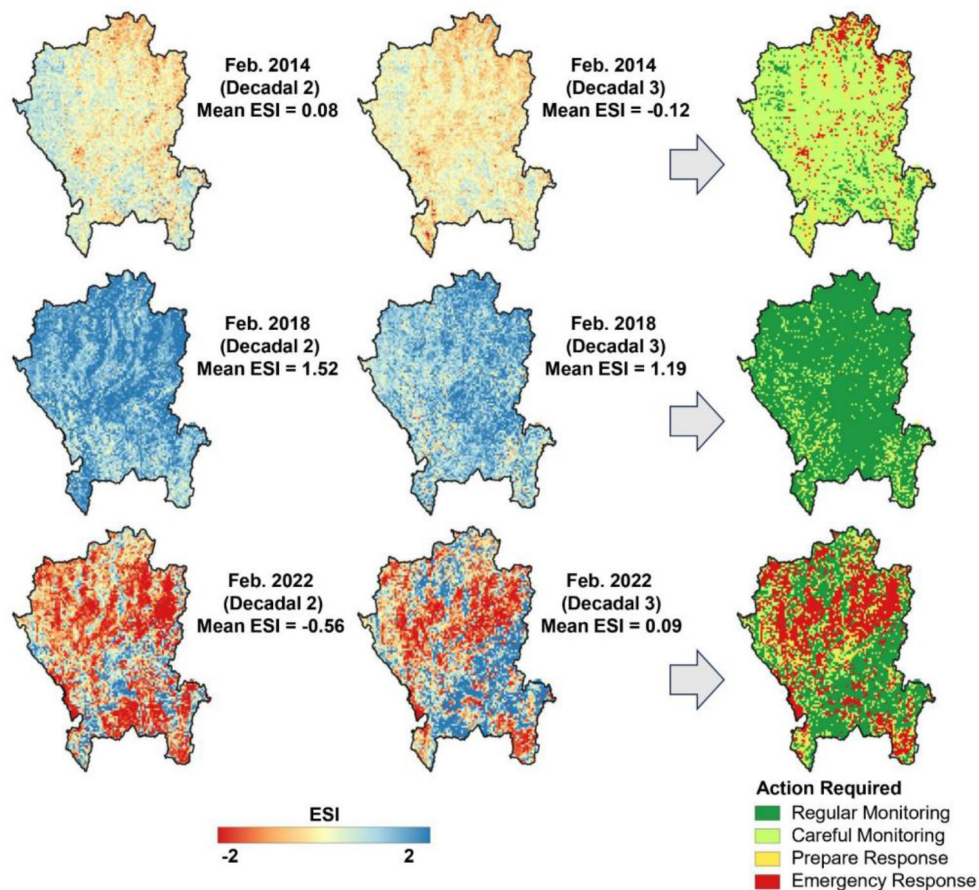


Fig. 4: Spatial distribution of the ESI and corresponding recommended actions across Northern Thailand.

based Evaporative Stress Index (ESI). Temporal analysis characterized drought patterns during 2012–2023, differentiating between short-term severe episodes and prolonged conditions. A key finding was the identification of persistent agricultural drought from late 2021 to early 2022, which was validated by independent ground-based and satellite observations despite prevailing La Niña conditions. This finding demonstrates ESI's capability for detecting actual agricultural impacts rather than relying solely on meteorological inputs.

Spatial analysis extended beyond detection by developing action-oriented maps based on consecutive 10-day ESI patterns. The classification system successfully identified localized stress areas masked by regional averages, enabling targeted resource allocation. The framework provided a tangible tool for prioritizing emergency response when integrated with exposure and resistance factors. Overall, this study advanced the application of ESI from a monitoring index to a practical component of an actionable drought management framework. The framework provides a foundation with strong potential for operational implementation in regions with complex terrain and limited ground-based monitoring that face similar data constraints and agricultural drought challenges. Future implementation would benefit from integrating complementary drought indices, validating against yield data and farmer surveys, and developing user interfaces to support real-time decision-making.

ACKNOWLEDGEMENT

The authors would like to thank the Thai Meteorological Department for providing meteorological data from weather stations in Northern Thailand.

Conflict of Interests: The authors declare that there is no conflict of interest regarding this study.

Funding: Faculty of Engineering at Kamphaeng Saen, Kasetsart University (Kamphaeng Saen Campus), Thailand

Data availability: TerraClimate Gridded ETo data can be downloaded from the Climatology Lab, UC Merced website at this URL: <https://www.climatologylab.org/terraclimate.html>. SSEBop Gridded ETa data can be downloaded from the FEWS NET USGS Data Portal website at this URL: <https://earlywarning.usgs.gov/fews/>. Meteorological data from weather stations in Northern Thailand may be provided by the corresponding author upon request.

Authors contribution: N. Boonpin: Conceptualization, Methodology, Data collection, Data analysis, Writing – original draft; P. Waiphara: Visualization and interpretation, Validation, Writing – review & editing; C. Chompuchan: Supervision, Conceptualization, Methodology, Visualization and interpretation, Validation, Writing – review & editing

REFERENCES

- Abatzoglou, J. T., Dobrowski, S. Z., Parks, S. A., & Hegewisch, K. C. (2018). TerraClimate, a high-resolution global dataset of monthly climate and climatic water balance from 1958-2015. *Scientific Data*, 5, 1–12. <https://doi.org/10.1038/sdata.2017.191>
- Amazirh, A., Chehbouni, A., Bouras, E. H., Benkirane, M., Ait Hssaine, B., & Entekhabi, D. (2023). Drought cascade lag time estimation across Africa based on remote sensing of hydrological cycle components. *Advances in Water Resources*, 182, 104586. <https://doi.org/10.1016/j.advwatres.2023.104586>
- Anderson, M. C., Norman, J. M., Mecikalski, J. R., Otkin, J. A., & Kustas, W. P. (2007). A climatological study of evapotranspiration and moisture stress across the continental United States based on thermal remote sensing: 2. Surface moisture climatology. *Journal of Geophysical Research Atmospheres*, 112, D11112. <https://doi.org/10.1029/2006JD007507>
- ASEAN Specialised Meteorological Centre. (2022). *ASMC Bulletin* (Issue 10). https://www.mss-int.sg/docs/default-source/rcc_bulletin_doc/asmc-bulletin-issue-no-10-sep-2022.pdf
- Chang, Q., Ficklin, D. L., Jiao, W., Denham, S. O., Wood, J. D., Brunsell, N. A., Matamala, R., Cook, D. R., Wang, L., & Novick, K. A. (2023). Earlier Ecological Drought Detection by Involving the Interaction of Phenology and Eco-Physiological Function. *Earth's Future*, 11, e2022EF002667. <https://doi.org/10.1029/2022EF002667>
- Fang, G. H., Yang, J., Chen, Y. N., & Zammit, C. (2015). Comparing bias correction methods in downscaling meteorological variables for a hydrologic impact study in an arid area in China. *Hydrology and Earth System Sciences*, 19(6), 2547–2559. <https://doi.org/10.5194/hess-19-2547-2015>
- Ha, T. V., Ureyen, S., & Kuenzer, C. (2023). Agricultural drought conditions over mainland Southeast Asia: Spatiotemporal characteristics revealed from MODIS-based vegetation time-series. *International Journal of Applied Earth Observation and Geoinformation*, 121, 103378. <https://doi.org/10.1016/j.jag.2023.103378>
- Hydro Informatics Institute. (2021). *Thailand Water Situation 2021*. <https://www.thaiwater.net/uploads/contents/current/YearlyReport2021/summary.html>
- Jeefoo, P. (2023). Thai Eastern Economic Corridor Drought Monitoring using Terra MODIS Satellite-based Data. *Geographia Technica*, 18(2), 123–131. <https://doi.org/10.21163/GT>
- Jeong, H., Park, H. S., Chowdary, J. S., & Xie, S. P. (2023). Triple-Dip La Niña Contributes to Pakistan Flooding and Southern China Drought in Summer 2022. *Bulletin of the American Meteorological Society*, 104(9), E1570–E1586. <https://doi.org/10.1175/BAMS-D-23-0002.1>
- Keune, J., Giuseppe, F. Di, Barnard, C., Damasio, E., & Wetterhall, F. (2025). ERA5 – Drought : Global drought indices based on ECMWF reanalysis. *Scientific Data*, 12, 616. <https://doi.org/10.1038/s41597-025-04896-y>
- Mergia, G. (2024). Spatiotemporal analysis of meteorological drought in El Niño years over Oromia region, Ethiopia. *Journal of Agrometeorology*, 26(1), 109–114. <https://doi.org/10.54386/jam.v26i1.2329>
- Northern Meteorological Center. (2022). *Chance of dry spells in Lampang Province using data from 2011 - 2020* (Technical Document No. 551.577.3-01-2022).
- Nurdiati, S., Sopaheluwakan, A., & Septiawan, P. (2022). Joint Pattern Analysis of Forest Fire and Drought Indicators in Southeast Asia Associated with ENSO and IOD. *Atmosphere*, 13, 1198. <https://doi.org/10.3390/atmos13081198>
- Otkin, J. A., Anderson, M. C., Hain, C., Mladenova, I. E., Basara, J. B., & Svoboda, M. (2013). Examining rapid onset drought development using the thermal infrared-based evaporative stress index. *Journal of Hydrometeorology*, 14(4), 1057–1074. <https://doi.org/10.1175/JHM-D-12-0144.1>
- Pei, W., Fu, Q., Liu, D., Li, T. xiao, Cheng, K., & Cui, S. (2018). Spatiotemporal analysis of the agricultural drought risk in Heilongjiang Province, China. *Theoretical and Applied Climatology*, 133, 151–164. <https://doi.org/10.1007/s00704-017-2182-x>
- Senay, G. B., Bohms, S., Singh, R. K., Gowda, P. H., Velpuri, N. M., Alemu, H., & Verdin, J. P. (2013). Operational Evapotranspiration Mapping Using Remote Sensing and Weather Datasets: A New Parameterization for the SSEB Approach. *Journal of the American Water Resources Association*, 49(3), 577–591. <https://doi.org/10.1111/jawr.12057>
- Sreeparvathy, V., Debdtut, S., & Mishra, A. (2025). A Review of Advances in Flash Drought Research: Challenges and Future Directions. *Earth's Future*, 13(8), e2025EF006603. <https://doi.org/10.1029/2025EF006603>
- Trisurat, Y., Alkemade, R., & Verburg, P. H. (2010). Projecting Land-Use Change and Its Consequences for Biodiversity in Northern Thailand. *Environmental Management*, 45(3), 626–639. <https://doi.org/10.1007/s00267-010-9438-x>
- USDA Foreign Agricultural Service. (2021). *Thailand rice: Recent dry conditions after a promising start; Optimism still remains for this crop season*. https://ipad.fas.usda.gov/cropexplorer/pecad_stories.aspx?regionid=sea&pubid=1237
- Wang, Q., Zeng, J., Qi, J., Zhang, X., Zeng, Y., Shui, W., Xu, Z., Zhang, R., Wu, X., & Cong, J. (2021). A multi-scale daily SPEI dataset for drought characterization at observation stations over mainland China from 1961 to 2018. *Earth System*

- Science Data*, 13(2), 331–341. <https://doi.org/10.5194/essd-13-331-2021>
- Yang, X., Shao, X., Mao, X., Li, X., & Li, R. (2019). An analysis of drought evolution characteristics based on standardized precipitation index : a case study in Southwest Guizhou Autonomous Prefecture , China. *Journal of Agrometeorology*, 21(3), 327–335. <https://doi.org/10.54386/jam.v21i3.255>
- Yoon, D., Nam, W., Lee, H., Hong, E., Feng, S., Wardlow, B. D., Tadesse, T., Svoboda, M. D., Hayes, M. J., & Kim, D. (2020). Agricultural Drought Assessment in East Asia Using Satellite-Based Indices. *Remote Sensing*, 12, 444. <https://doi.org/10.3390/rs12030444>
- Zaki, M. K., & Noda, K. (2022). A Systematic Review of Drought Indices in Tropical Southeast Asia. *Atmosphere*, 13, 833. <https://doi.org/10.3390/atmos13050833>